frontiers in
CELLULAR NEUROSCIENCE

ORIGINAL RESEARCH ARTICLE
published: 08 April 2010
doi: 10.3389/fncel.2010.00008

$GABA_A$ increases calcium in subventricular zone astrocyte-like cells through L- and T-type voltage-gated calcium channels

Stephanie Z. Young[1], Jean-Claude Platel[1], Jakob V. Nielsen[2], Niels A. Jensen[2] and Angélique Bordey[1]*

[1] *Departments of Neurosurgery and Cellular & Molecular Physiology, Yale University School of Medicine, New Haven, CT, USA*
[2] *Molecular Neurobiology Laboratory, Medical Biotechnology Center, University of Southern Denmark, Odense, Denmark*

Edited by:
Yehezkel Ben-Ari, INSERM, France

Reviewed by:
Enrico Cherubini, International School for Advanced Studies, Italy
Yehezkel Ben-Ari, INSERM, France

****Correspondence:***
Angélique Bordey, Department of Neurosurgery, Yale University School of Medicine, 333 Cedar Street, FMB 422, New Haven, CT 06520-8082, USA.
e-mail: angelique.bordey@yale.edu

In the adult neurogenic subventricular zone (SVZ), the behavior of astrocyte-like cells and some of their functions depend on changes in intracellular Ca^{2+} levels and tonic $GABA_A$ receptor activation. However, it is unknown whether, and if so how, $GABA_A$ receptor activity regulates intracellular Ca^{2+} dynamics in SVZ astrocytes. To monitor Ca^{2+} activity selectively in astrocyte-like cells, we used two lines of transgenic mice expressing either GFP fused to a Gq-coupled receptor or DsRed under the human glial fibrillary acidic protein (*hGFAP*) promoter. $GABA_A$ receptor activation induced Ca^{2+} increases in 40–50% of SVZ astrocytes. $GABA_A$-induced Ca^{2+} increases were prevented with nifedipine and mibefradil, blockers of L- and T-type voltage-gated calcium channels (VGCC). The L-type Ca^{2+} channel activator BayK 8644 increased the percentage of $GABA_A$-responding astrocyte-like cells to 75%, suggesting that the majority of SVZ astrocytes express functional VGCCs. SVZ astrocytes also displayed spontaneous Ca^{2+} activity, the frequency of which was regulated by tonic $GABA_A$ receptor activation. These data support a role for ambient GABA in tonically regulating intracellular Ca^{2+} dynamics through $GABA_A$ receptors and VGCC in a subpopulation of astrocyte-like cells in the postnatal SVZ.

Keywords: GABA, GABA receptors, stem cells, astrocyte, subventricular zone, neurogenesis, progenitor cells, proliferation

INTRODUCTION

Neurogenesis persists in two regions of the adult brain, the SVZ along the lateral ventricle and the subgranular zone in the hippocampal dentate gyrus (Lledo et al., 2006; Zhao et al., 2008). The SVZ contains a mosaic of cell types including neuroblasts ensheathed by cells with astrocytic features such as glial fibrillary acidic protein (GFAP) expression. A subpopulation of these GFAP-expressing cells (also called astrocyte-like cells or SVZ astrocytes) generates intermediate progenitors called transit amplifying cells. The latter generate neuroblasts that differentiate into interneurons in the olfactory bulb. Previous studies have shown that the distinct steps of neurogenesis (i.e. migration, proliferation and differentiation) are influenced by local molecules. These molecules differentially affect intracellular Ca^{2+} dynamics and regulate Ca^{2+}-dependent intracellular pathways (Bordey, 2006; Pathania et al., 2010). One such local molecule is the amino acid γ-aminobutyric acid (GABA) that is synthesized and released by SVZ neuroblasts as shown using immunohistochemistry for glutamic acid decarboxylase (GAD) (the enzyme that catalyzes the decarboxylation of glutamate to GABA) and GABA, and electrophysiology to show functional release from neuroblasts (Stewart et al., 2002; Nguyen et al., 2003; Bolteus and Bordey, 2004; De Marchis et al., 2004; Liu et al., 2005; Gascon et al., 2006; Platel et al., 2008).

GABA acts through specific receptors, $GABA_A$ receptors, which are expressed in both SVZ neuroblasts and astrocytes (Stewart et al., 2002; Nguyen et al., 2003; Wang et al., 2003b; Bolteus and Bordey, 2004; Liu et al., 2005). In developing systems, the $GABA_A$ receptor is thought to regulate the behavior of immature cells through depolarization leading to the canonical activation of VGCCs and intracellular Ca^{2+} increases (Owens and Kriegstein, 2002). Such a mechanism has been reported in SVZ neuroblasts and involves nifedipine-sensitive L-type VGCC (Nguyen et al., 2003; Wang et al., 2003b; Gascon et al., 2006). It has been speculated that this canonical Ca^{2+} increase may not operate in SVZ astrocytes due to their biophysical properties (low input resistance and hyperpolarized resting potential) (Liu et al., 2006; Bordey, 2007). We thus set out to investigate whether and, if so, how $GABA_A$ increases Ca^{2+} in SVZ astrocytes.

One limitation to address this issue has been the inability to distinguish Ca^{2+} indicator-loaded astrocyte-like cells from neuroblasts in acute SVZ slices. To study Ca^{2+} activity selectively in SVZ astrocytes, we used two lines of transgenic mice where astrocyte-like cells express intracellular DsRed or membrane-associated GFP. Using these mice revealed that traditional bath loading of Ca^{2+} indicators preferentially loaded neuroblasts at the slice surface while astrocyte-like cells resided deeper inside the tissue. Using pressure loading of a Ca^{2+} indicator dye inside the tissue, we preferentially loaded astrocyte-like cells. We found that a $GABA_A$ receptor agonist increased Ca^{2+} in a subset of astrocyte-like cells (~50%) through L- and T-type VGCCs. In addition, ambient GABA tonically regulated the frequency of Ca^{2+} activity in ~80% of SVZ astrocytes. GABA increased or decreased the frequency, subdividing the SVZ astrocytes into two subpopulations. For the first time this finding illustrates a functional difference among astrocyte-like cells of the SVZ. Such a $GABA_A$-regulation in selective astrocyte-like cells may impact Ca^{2+}-dependent mechanisms, including proliferation and the release of diffusible molecules (e.g. ATP; Striedinger et al., 2007).

MATERIALS AND METHODS

ANIMALS

Experiments were performed in several lines of transgenic mice: (1) Mice expressing DsRed under the human *GFAP* promoter (*hGFAP*-DsRed mice) were produced by the co-authors, N.A. Jensen and J.V. Nielsen (Noraberg et al., 2007). To generate the *hGFAP*-DsRed transgene, the pDsRed2-1 plasmid (Clontech) was initially modified to introduce a *Pac*I site downstream of the SV40 polyadenylation signal, by filling in an *Afl*II site. Subsequently, the *hGFAP* promoter (Brenner et al., 1994) was cloned into the *Bgl*II and *Sal*I sites, before a rabbit β-globin intron was inserted into the *Bam*HI sites between the *hGFAP* promoter and the DsRed coding sequence. For microinjection, the transgene was excised from the plasmid backbone by digestion with *Bgl*II and *Pac*I, gel-purified and microinjected, at a concentration of 6 ng/μl, into the pronucleus of fertilized B6D2F1 mouse eggs as previously described (Nielsen et al., 2007). Transgenic *hGFAP*-DsRed mice were identified by PCR with primers: 5′-TCTGGGCACAGTGACCTCAGTG and 5′-GGGACATCTTCCCATTCTAAAC. (2) *hGFAP*-DsRed mice were crossed with homozygote mice carrying GFP under the doublecortin promoter (*DCX*-GFP mice, FVB/N strain, a gift from Dr. R. Miller, University of Chicago, originally from Gensat) to generate *hGFAP*-DsRed/*DCX*-GFP mice. These mice were used in 25% of the experiments instead of *hGFAP*-DsRed mice. (3) *hGFAP-tTA/TetO*-MrgA1:GFP mice (called *hGFAP*-MrgA1:GFP mice) were a gift from Dr. Ken McCarthy (University of North Carolina at Chapel Hill). In the absence of doxycycline, astrocytes express MrgA1 receptors fused to GFP (Fiacco et al., 2007). All experimental protocols were approved by the Institutional Animal Care and Use Committees of Yale School of Medicine and by the Danish National Animal Care and Use Committee. Mice were used between postnatal day (P) 20 and P42.

IMMUNOHISTOCHEMISTRY

Slice preparation, immunostaining, and image acquisition and analysis were as previously described (Platel et al., 2009). Primary antibodies included: anti-DCX (goat or rabbit, 1:100, Santa Cruz, SC8066 and SC28939), anti-GFAP (rabbit, 1:1000, Dako, Z0334), anti-EGFR (sheep, 1:100, Millipore, 06-129), and anti-GFP (chicken, 1:500, Abcam). Each staining was replicated at least in four to five slices from three different mice. The appropriate secondary antibodies were Alexa fluor series (1:1000, Invitrogen, USA) or Cyanine series (1:500, Jackson Labs). Z-section images (spaced by 1–2 μm over 10–20 μm) were acquired on a laser-scanning confocal microscope (Olympus FluoView 1000) with a 20× dry objective (N.A. 0.75) or a 60× oil objective (N.A. 1.42). Images were analyzed using Imaris 4.0 (Bitplane AG, Switzerland) and reconstructed in ImageJ 1.39t (Freeware, Wayne Rasband, NIH, USA) and Photoshop CS3 (Adobe, USA).

ACUTE SLICE PREPARATION AND PATCH CLAMP RECORDINGS

Acute coronal or sagittal brain slices (250–300 μm-thick) containing the SVZ were prepared as we previously described (Bolteus and Bordey, 2004; Bolteus et al., 2005). Slices were placed in a flow-through chamber and continuously superfused with oxygenated artificial cerebrospinal fluid (aCSF) containing (in mM): NaCl 125; KCl 2.5; $CaCl_2$ 1.8; $MgCl_2$ 1; $NaHCO_3$ 25; glucose 10. Experiments were performed on an upright Olympus BX61WI microscope equipped with an Olympus FluoView 1000 confocal microscope and a water-immersion Nomarski phase-contrast and fluorescence 60× objective (N.A. 0.9).

Whole-cell patch clamp recordings were obtained as previously described (Wang et al., 2003a,b; Bolteus and Bordey, 2004; Liu et al., 2006). Pipettes had resistances of 6–8 MΩ when filled with an intracellular solution containing the following: 110 mM KCl, 1.0 mM $CaCl_2$, 10 mM EGTA, 10 mM HEPES, 50 μM Alexa Fluor 488 dye and an ATP-regenerating solution that included 4 mM K_2ATP, 20 mM K_2-phosphocreatine, 50 U/ml creatine phosphokinase, and 6 mM $MgCl_2$. The pH and the osmolarity were adjusted to 7.2 and 290 mOsm, respectively. The liquid junction potential (~4 mV) was not corrected. Whole-cell recordings were performed using an Axopatch 200B amplifier, and current signals were low-pass filtered at 2–5 kHz and digitized on-line at 5–20 kHz using a Digidata 1320 digitizing board (Axon Instruments, Foster City, CA, USA). Recorded cells were held at −60 mV. Voltage steps were applied from −100 to +100 mV by 20 mV increment. Capacitive and leak currents were not subtracted.

CALCIUM IMAGING

SVZ cells were loaded by pressure application of Fluo-4 AM (100 μM in aCSF, 0.4% Pluronic acid F-127, Invitrogen). We observed no differences in data obtained with either *hGFAP*-DsRed or *hGFAP*-MrgA1:GFP mice regarding the pharmacology of muscimol responses; we therefore pooled the data. Images were acquired every 2 s with FluoView acquisition software. In acute slices from *hGFAP*-MrgA1:GFP mice, Fluo-4 AM-astrocyte-like cells were distinguished from other SVZ cells due to their enhanced green fluorescence on their cell membrane. In addition, application of a selective peptide agonist of MrgA1 receptors (that has no endogenous receptors) was routinely used to induce Ca^{2+} responses selectively in SVZ astrocytes to identify them at the end of the experiments. ROIs were placed on SVZ cells that responded to the peptide during a 10–20 s application period.

For spontaneous movies, images were acquired every 2 s (0.5 Hz) for 10 min in each condition with 5 min of wash-in or wash-out between each movie. F_0 (i.e. baseline) and F are the mean fluorescence intensities measured throughout all of the regions of interest (ROIs) and in each ROI, respectively. A change in fluorescence was considered to be a Ca^{2+} increase if it was >15% F/F_0 increase. Intracellular Ca^{2+} changes were calculated using Calsignal (Platel et al., 2007) and Clampfit 10. F/F_0 was detected with Calsignal and traces were exported into Clampfit for peak analysis using the threshold detection function. For peak analysis, the baseline for each ROI trace was manually adjusted to zero. In addition, traces from control and drug-treated movies were concatenated and the same threshold for peak detection was used. ROIs were designated as "responding" if the cell was responsive at least 50% of muscimol applications in order to perform subsequent pharmacology. "Non-responsive" cells were cells that displayed no increase in F/F_0.

Data are expressed as mean ± standard error. Statistical analysis used a two-tailed *t*-test except where noted.

PHARMACOLOGY

Ca^{2+} imaging experiments were performed in the presence of the $GABA_B$ blocker CGP 52432 (1 μM) and blockers of glutamate receptors including D-APV (50 μM) for NMDA receptors, NBQX

(20 μM) for AMPA/kainate receptors, MPEP (10 μM) and JNJ 16259685 (100 nM) for group I metabotropic glutamate receptors. We also used for selective experiments: nickel (100 μM) to block N- and R-type VGCCs; nifedipine (10 μM, Sigma-Aldrich) and mibefradil dihydrochloride (10 μM) for blocking L-type and T-type VGCCs, respectively; BayK 8644 (10 μM) to enhance L-type VGCC activity; 2-aminoethoxydiphenyl borate 2-APB (100 μM) for blockade (although non-selective) of IP_3-related signaling. Drugs were from Tocris Biosciences (MO, USA), except where noted.

RESULTS

CHARACTERIZATION OF DsRED-POSITIVE CELLS IN THE SVZ OF *hGFAP*-DsRED MICE

We first verified that DsRed is expressed in astrocyte-like cells of the SVZ. We immunostained for GFAP (blue) in sections from *hGFAP*-DsRed/*DCX*-GFP mice (**Figures 1A,B**). We observed bright DsRed-positive cells, which were GFAP-positive (arrows in **Figure 1B**), and some faint DsRed cells, which were GFAP-negative and *DCX*-GFP-positive (arrowhead in **Figure 1B**). This result was confirmed by staining for both GFAP and DCX in sections from *hGFAP*-DsRed mice (**Figure S1** in Supplementary Material). DsRed-positive cells occasionally stained positive for the transit amplifying cell marker epidermal growth factor receptor (EGFR, **Figure S1B** in Supplementary Material, arrowhead). The known half-life of DsRed (~4 days) allows it to persist at a lower level in daughter cells. These findings are thus in agreement with GFAP-positive cells (*i.e.* SVZ astrocytes) being neural progenitors that generate EGFR-cells and neuroblasts (Doetsch et al., 2002; Platel et al., 2009).

We next performed patch clamp recordings of DsRed-fluorescent cells in acute slices where cells with different fluorescence intensity could be observed (**Figures 1C,D**). Every bright DsRed-fluorescent cell recorded had a hyperpolarized resting potential (mean of −80.8 ± 1.0 mV), low input resistance (57.4 ± 9.1 MΩ, $n = 7$), and a linear current–voltage relationship following depolarizing steps (from −160 to +100 mV, **Figures 1E,F**) from a holding potential of −80 mV. Thus, bright DsRed-fluorescent have characteristics of

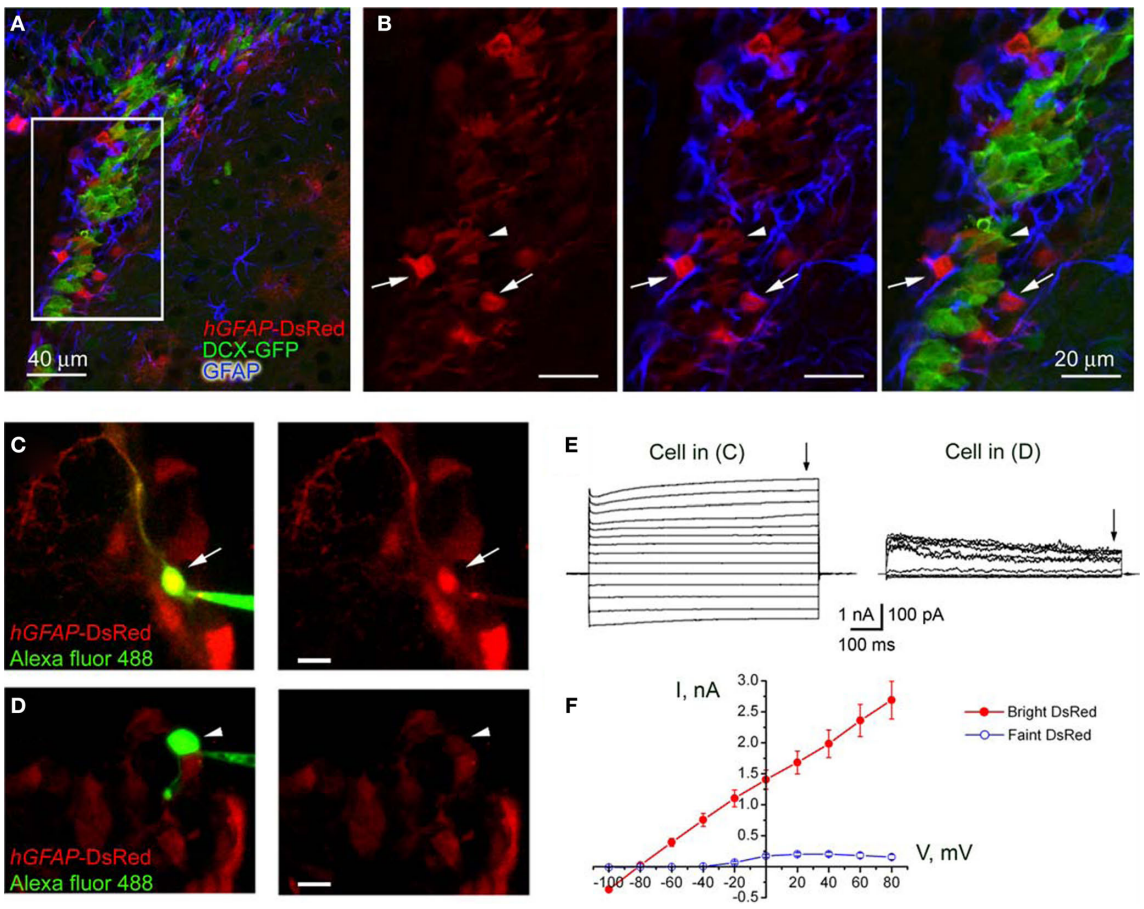

FIGURE 1 | Characterization of *hGFAP*-DsRed-fluorescent cells in the SVZ. **(A)** Confocal images (one optical section) of GFAP immunostaining (blue) in the SVZ contained in a section from a *hGFAP*-DsRed/*DCX*-GFP mouse (P30). **(B)** Higher power photographs of the staining shown in the white square in (A). The arrows point to GFAP-positive DsRed-fluorescent cells while the arrowhead points to GFAP-negative, GFP-fluorescent neuroblasts. **(C and D)** Photographs of Alexa fluor 488-filled bright (C) and faint (D) red cells during patch clamp recording in acute slices from *hGFAP*-DsRed mice. Scale bar: 15 μm. **(E)** Traces of whole cell currents obtained from the cells shown in (C, bright red) and (D, faint red). The cells in (C) and (D) display the current profiles of a GFAP-progenitor and a neuroblast, respectively. **(F)** Mean current–voltage relationships (measured at the end of the voltage steps, arrows in E) of bright cells (red filled circles, $n = 6$) and faint cells (blue open circles, $n = 5$) give reversal potentials of –81 and –43 mV, respectively.

astrocytes of the SVZ (Liu et al., 2006). By contrast, every recorded, faint DsRed-fluorescent cell displayed characteristics of neuroblasts (Wang et al., 2003a; Bolteus and Bordey, 2004). These characteristics include high input resistance (mean of 4.4 ± 1.3 GΩ), depolarized zero-current resting potentials (−42.7 ± 8.7 mV, $n = 5$), and the presence of voltage-dependent outward currents (**Figures 1E,F**). These data suggest that bright and faint DsRed-fluorescent cells can be unambiguously identified as astrocyte-like cells and neuroblasts, respectively, in acute slices.

GFP-POSITIVE CELLS IN THE SVZ OF *hGFAP*-MRGA1:GFP MICE ARE ASTROCYTE-LIKE CELLS

One important limitation of the *hGFAP*-DsRed mice for performing Ca^{2+} imaging is the fact that not every astrocyte-like cell is DsRed-fluorescent (**Figures 1A,B**). This is more apparent in sections from *hGFAP*-DsRed mice crossed with *hGFAP*-GFP mice. While some DsRed-fluorescent cells are GFP-positive (arrows), not all GFP-positive cells are DsRed-fluorescent (arrowheads, **Figures 2A–C**). We thus acquired transgenic mice that express an exogenous Gq-protein coupled receptor (called Mas-related gene A1, MrgA1) in GFAP-expressing cells (*i.e.* astrocytes). MrgA1 has no endogenous ligand in the brain (Fiacco et al., 2007). The MrgA1 receptor fused to GFP was targeted to astrocytes using the inducible tet-off system. Mice expressing the tetracycline transactivator (tTA) under the human *GFAP* promoter were crossed to mice in which the MrgA1:GFP receptor was transcribed using the tet-off (tetO) minimal promoter. In the SVZ of *hGFAP*-tTA/tetO-MrgA1:GFP mice (referred henceforth as *hGFAP*-MrgA1:GFP mice), GFP displays a membrane expression selectively in all astrocyte-like cells (GFAP+ cells, red) but not in neuroblasts (DCX+ cells, blue, **Figures 2D,E**). In addition, SVZ astrocytes loaded with the Ca^{2+} indicator dye Fluo-4 AM can be further identified with a peptide agonist for MrgA1 receptors that does not bind endogenous receptors in the brain. Pressure application of phe-leu-arg-phe amide peptide (FLRFa, 50 μM, 10–20 s) induced Ca^{2+} increases in GFP-decorated cells, i.e. astrocyte-like cells (**Figures 2F,G**).

GABA$_A$ RECEPTOR ACTIVATION LEADS TO CA^{2+} INCREASES IN SVZ ASTROCYTES THROUGH VGCCs

We previously reported that astrocyte-like cells express functional GABA$_A$ receptors using patch clamp recordings (Liu et al., 2005). However, it remained unknown whether these receptors led to Ca^{2+} increases in these cells. We pressure loaded slices with Fluo-4 AM in slices from *hGFAP*-DsRed and *hGFAP*-MrgA1:GFP mice (**Figures 3A,E**, respectively). Application of the GABA$_A$ receptor agonist muscimol (50 μM, 5 s) increased Ca^{2+} in 38.1 ± 4.8% and 51.3 ± 3.5% of SVZ astrocytes from *hGFAP*-DsRed and *hGFAP*-MrgA1:GFP mice (106 cells, $n = 17$ slices and 396 cells, 16 slices, respectively, **Figures 3B,D,F**). Experiments were performed in the presence of glutamate and GABA$_B$ receptor blockers (see Materials and Methods). GABA$_A$-induced Ca^{2+} responses were abolished by either bicuculline or picrotoxin (50 μM), two GABA$_A$ receptor antagonists, in 94 ± 4.67% of the muscimol-responding cells (27 cells, $n = 5$ slices total, **Figures 3C,G and 4E,F**).

GABA$_A$ receptor activation is known to depolarize parenchymal astrocytes (Barakat and Bordey, 2002; Bekar and Walz, 2002). Following GABA$_A$ receptor-induced depolarization, intracellular Ca^{2+} increases in immature cells are also thought to result from the canonical activation of VGCCs (Owens and Kriegstein, 2002; Meier et al., 2008). We thus tested the effects of three VGCC blockers on the percentage of SVZ astrocytes displaying muscimol-induced Ca^{2+} increases in slices from both *hGFAP*-DsRed and *hGFAP*-MrgA1:GFP mice. VGCCs are grouped into three families: (1) the high-voltage activated dihydropyridine (DHP)-sensitive channels (L-type, $Ca_V1.x$), (2) the high-voltage activated DHP-insensitive channels (P-, N- and R-type, $Ca_V2.x$), and (3) the low-voltage activated channels (T-type, $Ca_V3.x$). We tested the following three blockers: Nickel (Ni^{2+}, 100 μM) for R-type $Ca_V2.3$ and T-type $Ca_V3.2$ channels (high sensitivity), and for other T-type channels (low-sensitivity); the DHP antagonist nifedipine (10 μM) for L-type channels, and mibefradil (10 μM) for T-type channels. Ni^{2+} significantly decreased the percentage of muscimol-responding astrocytes but by only 30 ± 9.4% ($n = 50$ cells, six slices, **Figures 4E,F**). Nifedipine and mibefradil significantly decreased the percentage of muscimol-responding astrocytes by 61 ± 10% **Figures 4A,B** and 48 ± 4%, respectively ($n = 217$ cells, six slices, and 78 cells, four slices, respectively, **Figures 4E,F**). When used together, these three VGCC blockers abolished muscimol responses in 90 ± 4% of the responding SVZ astrocytes (**Figures 4E,F**). Of the cells that continue to respond, none of these drugs had any effect on the amplitude or area of the Ca^{2+} responses (**Figure 4G**). These data suggest that GABA$_A$-induced Ca^{2+} responses in astrocyte-like cells of the SVZ are predominately mediated by Ca^{2+} influx through L- and T-type VGCCs.

As illustrated in **Figures 3D and 4E**, 40–50% of SVZ astrocytes display Ca^{2+} increases in response to GABA$_A$ receptor activation. Considering that nearly all SVZ astrocytes tested have been reported to display functional GABA$_A$ currents (Liu et al., 2005), the lack of Ca^{2+} responses could be due to either the absence of functional VGCCs or the fact that GABA$_A$ depolarization does not reach VGCC threshold. We thus tested the L-type VGCC activator BayK 8644. In the presence of BayK 8644, there was a significant increase (to 190% of control) in the % of cells responding to muscimol (from ~35% to 75%, **Figures 4C,D,E,F**). These data suggest that most astrocyte-like cells express DHP-sensitive VGCCs. BayK 8644 also increased the area, but not the amplitude, of muscimol-induced Ca^{2+} increases (**Figure 4G**), suggesting that BayK 3644 prolonged Ca^{2+} responses due to GABA$_A$ receptor activation.

Considering that increases in intracellular Ca^{2+} can further trigger Ca^{2+} increases from intracellular stores, we tested 2-APB, a blocker of inositol-1,4,5-trisphosphate receptors (IP3) and IP3-sensitive intracellular stores, among other channels at 100 μM (Bootman et al., 2002; Peppiatt et al., 2003). Bath application of 2-APB resulted in a 30 ± 9% decrease in the number of muscimol-responding astrocytes, but this decrease was not significant (**Figures 4E,F**, t-test, $p > 0.05$). Nevertheless, when analyzing cells that continue to respond after drug application, 2-APB significantly reduced the amplitude and area of muscimol-induced Ca^{2+} transients, while nifedipine and other VGCC blockers did not (**Figure 4G**). These data suggest that Ca^{2+} release from intracellular stores contributes to the increase in intracellular Ca^{2+} concentration following GABA$_A$ depolarization-induced Ca^{2+} influx through VGCCs.

AMBIENT GABA CONTROLS THE FREQUENCY OF BASELINE CA^{2+} ACTIVITY IN SVZ ASTROCYTES

We previously reported that 60% of SVZ astrocytes recorded with the patch clamp technique displayed a tonic current due to GABA$_A$ receptor activation (Liu et al., 2005). We thus examined whether

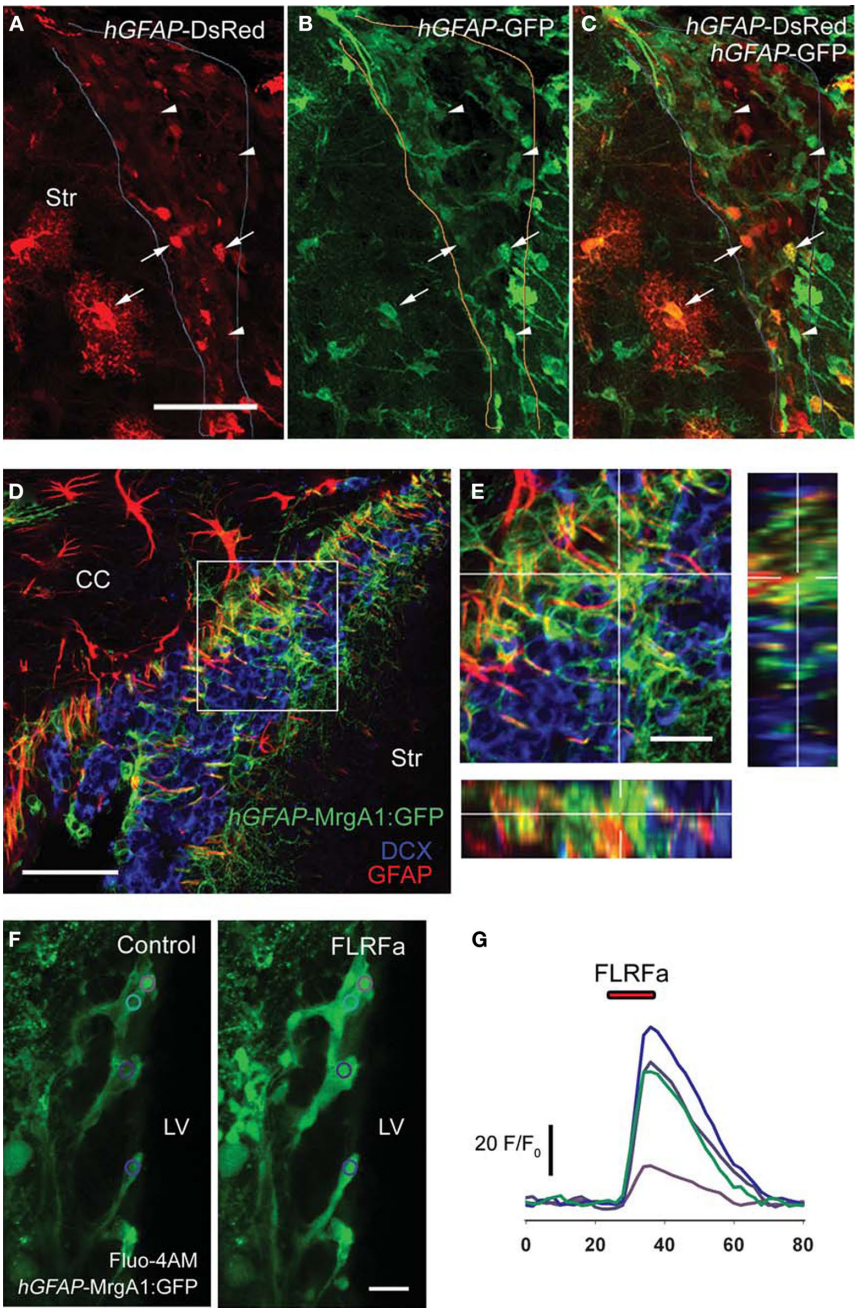

FIGURE 2 | Characterization of *hGFAP*-tTA-MrgA1:GFP mice in the SVZ. **(A–C)** Confocal z-section of a slice from a *hGFAP*-tTA-MrgA1:GFP/*hGFAP*-DsRed mouse. The arrows point to SVZ astrocytes that are both DsRed and GFP-fluroescent, while the arrowheads point to astrocytes that are only GFP-positive. Scale bar = 30 μm. **(D)** A confocal z-stack (four images, spaced by 1.5 μm) of a slice from a *hGFAP*-tTA-MrgA1:GFP mouse. Astrocytes express the MrgA1:GFP. GFP signal colocalized with GFAP (red) but does not colocalize with neuroblast marker DCX (blue). Scale bar = 30 μm **(E)** Higher power image of region indicated by a white box in (D). Scale bar = 10 μm. **(F)** Confocal images of Fluo-AM-loaded slice from a *hGFAP*-tTA-MrgA1:GFP mouse before and during peptide FLRFa application. Regions of interest (ROIs) are indicated by colored circles. Scale bar = 10 μm **(G)** Traces showing F/F_0 from ROIs in (*F*), analyzed in CalSignal. CC = corpus callosum, Str = striatum.

ambient GABA exerted a tonic regulation of Ca^{2+} dynamics in SVZ astrocytes. Recordings were performed in the presence of blockers of GABA$_B$ and glutamate receptors, as described in the Methods. We found that 77.8% of astrocyte-like cells displayed baseline Ca^{2+} activity in the form of Ca^{2+} transients at an average frequency of 0.252 Hz (10 min of recordings, $n = 196$ cells, four slices, see traces in control conditions in **Figure 5D**). To test the effect of drugs on Ca^{2+} activity, a 10-min recording was following by a 5-min drug wash-in and an additional 10-min recording in the presence of the drug. With no drug application (control movies), spontaneous Ca^{2+} activity was

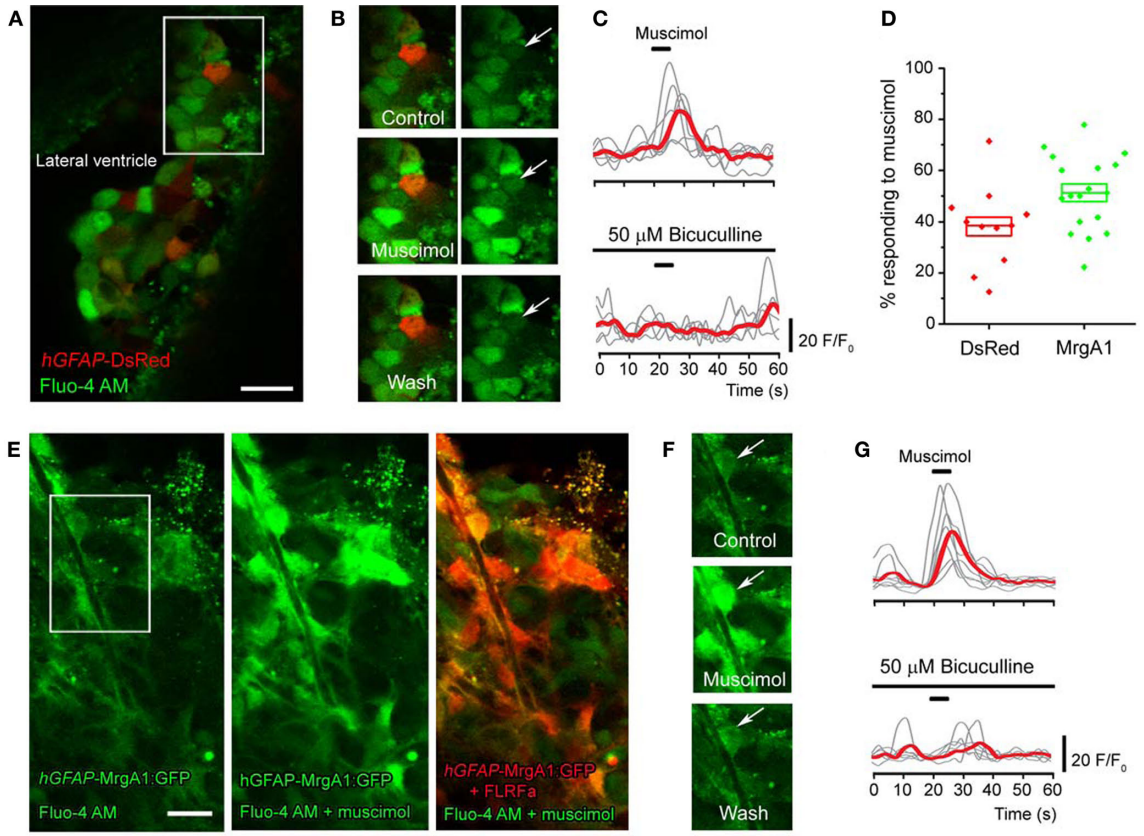

FIGURE 3 | GABA$_A$ receptors regulate Ca^{2+} dynamics in SVZ astrocytes. **(A)** Z-stack confocal image (six images spaced by 1.5 μm) of Fluo-4 AM loaded SVZ cells in a coronal slice from a *hGFAP*-DsRed mouse. Scale bar = 10 μm. **(B)** Confocal image of the same cells shown in the white square in (A) under control conditions, during and following muscimol application. The arrow points to the DsRed-fluorescent cell, which responded to muscimol. **(C)** Representative muscimol-induced Ca^{2+} responses under control and in the presence of bicuculline (a GABA$_A$ receptor blocker). The red trace represents the average of the individual gray traces (n = 7 cells). **(D)** Box plots of the percentage of GFAP-progenitors responding to muscimol in *hGFAP*-DsRed or *hGFAP*-MrgA1:GFP mice (n = 9 and 17 slices, respectively). Box: SEM, bar: median, diamonds: individual slice values. **(E)** Confocal image (one optical section) of Fluo-4 AM loaded SVZ cells (green) in a sagittal slice from a *hGFAP*-MrgA1:GFP mouse. Second panel shows SVZ cells responding to muscimol. The last panel is an overlay of images from responses to FLRFa peptide (orange, indicating SVZ astrocytes) and muscimol (green). Scale bar = 10 μm. **(F)** Confocal image of the same cells shown in the white square in (E) under control conditions, during and following muscimol application. The arrow points to the MrgA1:GFP-fluorescent, FLRFa-responsive cell, which also responded to muscimol. **(G)** Representative muscimol-induced Ca^{2+} responses under control and in the presence of bicuculline in cells from *hGFAP*-MrgA1:GFP slices. The red trace represents the average of the individual gray traces (n = 8 cells).

stable over time. Following analysis of Ca^{2+} frequency in the first and second 10-min periods, we found that 26.3 ± 4.8% and 19.0 ± 2.5% of the cells displayed a non-significant increase and decrease in the frequency of Ca^{2+} transient to 117.0 ± 6.3% and 81.7 ± 6.8% of control, respectively (n = 47 cells, three slices). Spontaneous Ca^{2+} activity was eliminated following 15–20 min of 2-APB application (data not shown), as expected, since regenerative Ca^{2+} transients have been shown to involve Ca^{2+} from internal stores that rely on the activation of IP3 receptors in various cell types (D'Andrea et al., 1993; Ciapa et al., 1994; Liu et al., 2001; Bellamy, 2006). When recorded in the presence of bicuculline (Bic) under baseline conditions, wash-out of bicuculline had two distinct effects on SVZ astrocytes. In 79 ± 3% of the astrocyte-like cells bicuculline wash-out resulted in a significant increase in the frequency of Ca^{2+} transients to 216 ± 39% of control (from 0.154 to 0.36 Hz, n = 90 cells, **Figures 5A,B**, $p < 0.01$). In addition, in 18 ± 6% of the SVZ astrocytes bicuculline wash-out resulted in a significant decrease in the frequency of Ca^{2+} transients to 72.9 ± 4.6% of control (from 0.45 to 0.34 Hz, n = 15/90 cells, **Figure 5B**). Wash-out of SR-95531 (gabazine, 100 nM), a non-competitive GABA$_A$ receptor antagonist, had similar effects (data not shown). Gabazine wash-out increased and decreased the frequency of Ca^{2+} transients in 41% and 27% of the SVZ astrocytes, respectively (n = 3 slices, data not shown). Bath application of bicuculline had the opposite effects to that of bicuculline wash-out, as expected. Bicuculline wash-in significantly decreased the frequency of Ca^{2+} transients to 60 ± 6% of control in 46 ± 8% of astrocyte-like cells (from 0.252 to 0.175 Hz, n = 185 cells) and increased the frequency to 223 ± 32% of control in 31 ± 3% of the cells in the same slices (from 0.10 to 0.25 Hz, n = 185 cells, four slices, **Figures 5C,D**, $p < 0.05$).

DISCUSSION

In this study we first report the use of two transgenic mouse lines to perform Ca^{2+} imaging in astrocyte-like cells of the SVZ. Without these mice, identifying Fluo-4 AM-loaded astrocytes among other

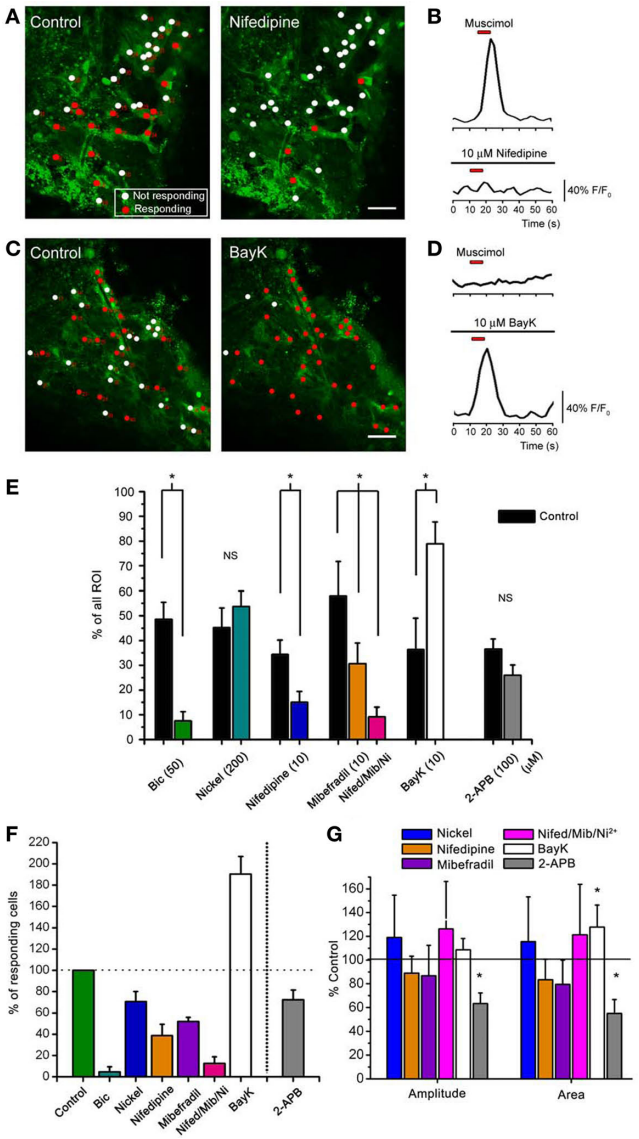

FIGURE 4 | Muscimol responses in SVZ astrocytes are inhibited by L- and T-type Ca^{2+} channel blockers. (A,C) Confocal images of Fluo-4 AM-loaded sagittal slices from *hGFAP*-MrgA1:GFP mice in control and in the presence of nifedipine in (A) (10 µM, an L-type Ca^{2+} channel blocker) or BayK in **(C)** (10 µM, a L-type Ca^{2+} channel enhancer). The red circles indicate muscimol-responsive SVZ astrocytes; the white circles indicate non-responsive cells. More cells respond to muscimol in the presence of BayK (indicated by red circles) while nifedipine silences cells. **(B)** Representative muscimol-induced Ca^{2+} responses from a "responding" cell (red circle) and subsequent block by nifedipine. **(D)** Representative muscimol-induced Ca^{2+} responses after bath application of BayK from a previously "non-responding" cell (white circle). Red bar: 10 s muscimol (20 µM). **(E)** Bar graphs showing the % of cells responding to muscimol from total ROI analyzed. Bic: bicuculline. **(F)** Bar graphs of the % of active cells responding after drug treatment. **(G)** Bar graphs of % of control of amplitude and area from cells that continued to respond after drug treatment. NS = not significant, * = $p < 0.05$.

SVZ cells was not feasible. *hGFAP*-DsRed mice are the most practical mouse line for performing Ca^{2+} imaging with the green fluorescent dye Fluo-4 AM since DsRed fluorescence is readily distinguishable from Fluo-4 fluorescence. However, in these mice not every SVZ astrocyte fluoresces red, and it is unclear whether a sub-population is targeted. In addition, the long half-life of DsRed could be an issue for positive identification. Newly born neuroblasts are DsRed fluorescent but are dimmer than astrocytes. The *hGFAP*-MrgA1:GFP mouse line appears to be the best model to study Ca^{2+} activity in SVZ astrocytes. GFP being fused to the MrgA1 receptor highlights the cell membrane and appears brighter than cytoplasmic Fluo-4 AM-loading. In addition, and perhaps more importantly, SVZ astrocytes can be selectively identified following increases in intracellular Ca^{2+} using the FLRFa peptide. In our system bath loading of the Ca^{2+} indicator Fluo-4 AM resulted in surface labeling of neuroblasts (data not shown). In the SVZ, cells are densely packed, thus limiting dye diffusion inside the tissue. In addition, neuroblasts tend to "bulge out" of the slice surface while astrocytes remain anchored inside the tissue as previously reported (Wang et al., 2003a). Instead, we used pressure loading inside the tissue resulting in preferential loading of SVZ astrocytes. With these experiments, we recommend using *hGFAP*-MrgA1:GFP mice to study Ca^{2+} activity in astrocyte-like cells of the SVZ in future studies.

Next, our pharmacological analyses suggest that the GABA$_A$-mediated Ca^{2+} increases arise from Ca^{2+} influx through L- and T-type VGCCs that are then amplified by Ca^{2+}-induced Ca^{2+} release from internal stores possibly involving IP3 receptors. This pathway is well-described in other neuronal and non-neuronal cell populations, and implies that GABA$_A$ receptor activation results in membrane depolarization that, in turn, activates VGCCs. Indeed, astrocytes are known to be depolarized by GABA$_A$ receptor activation resulting in GABA$_A$-induced Ca^{2+} increases (Bekar and Walz, 2002; Meier et al., 2008). GABA$_A$ depolarization is likely due to high intracellular Cl^- in SVZ astrocytes, although expression of the Cl^- importing transporter $Na^+/K^+/2Cl^-$ (NKCC1) and importantly the absence of the exporting Cl^- transporter $K^+/2Cl^-$ (KCC2) have not been examined in SVZ cells.

Considering the low-activation threshold of T-type VGCCs (as low as −70 mV) (Nilius et al., 2006), it is easily conceivable that these VGCCs can be opened by GABA$_A$-induced depolarization based on the published biophysical properties of SVZ astrocytes. Indeed, GABA$_A$ currents (100 µM GABA) range from −20 to −400 pA in gap-junction coupled SVZ astrocytes held at −84 mV (Liu et al., 2005). The current has a mean of −60 pA in SVZ astrocytes recorded in the presence of a gap junction channel blocker (unpublished data). These cells were recorded with an intracellular solution containing near-physiological chloride concentration. SVZ astrocytes' mean input resistance is 250 MΩ (range from 50 to 500 MΩ) and their mean resting potential is −85 mV ranging from −73 to −95 mV (Liu et al., 2006). Thus, a 60-pA GABA$_A$-current in a 250-MΩ astrocyte would result in a 15-mV depolarization, which is sufficient to reach the threshold for T-type VGCC activation.

L-type VGCCs are high-voltage activated ranging between −50 and −40 mV (Lacinova, 2005). Around ~40–50% of total astrocytes are muscimol-responsive in control conditions (from **Figure 3E**). Of those, ~40% are nifedipine-sensitive (see **Figure 4F**). Therefore, the population of astrocytes that reach the threshold for activation by L-type VGCCs comes to ~16–20% of all SVZ astrocytes. Similarly, SVZ astrocytes with higher input resistances (above 250 MΩ) correspond to ~40% of the total SVZ astrocytes (see Figure 6 in Liu et al., 2006). Of those with higher input resistance, 20% also have

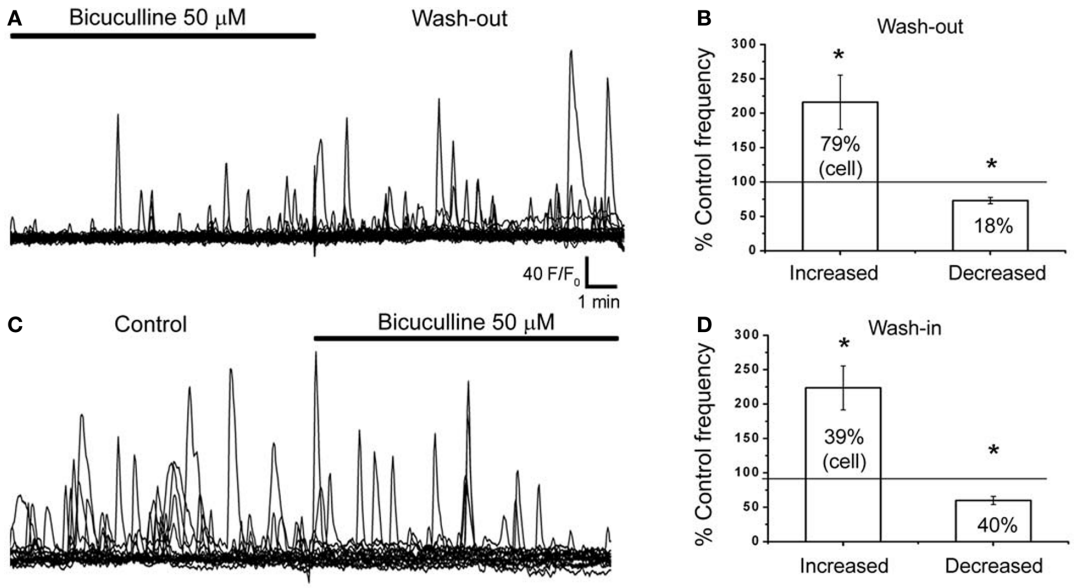

FIGURE 5 | Spontaneous Ca^{2+} activity in SVZ astrocytes are sensitive to GABA$_A$ receptor inhibition. (A,C) Representative traces of spontaneous Ca^{2+} activity from SVZ astrocytes before and after bicuculine (50 μM) wash-out **(A)** or wash-in **(C)**. **(B)** Bar graphs showing that 79% of SVZ astrocytes show an increased frequency to 220% of control during bicuculline wash-out. **(D)** Bar graphs showing that during bicuculline wash-I, 40% of SVZ astrocytes show a decreased 60% in frequency to compared to control. *indicates statistical significance.

resting potentials more depolarized than −80 mV, both of which would be required to reach L-type VGCC activation threshold. In this population, a current of 120 pA or less will be sufficient to reach the activation threshold of L-type VGCCs.

In the non-responding SVZ astrocytes, it is possible that either these cells do not express functional VGCCs or that GABA$_A$-depolarization did not reach the activation threshold for VGCCs. The fact that in the presence of BayK 8644, three-quarters of the SVZ astrocytes responded to muscimol suggests that the majority of, and perhaps all, astrocyte-like cells expresses DHP-sensitive VGCCs. These data suggest that GABA$_A$-depolarization in non-responding astrocyte-like cells does not reach the threshold to open VGCCs.

A question associated with the above data is whether there is enough GABA in the ambient milieu to activate GABA$_A$ receptors and modulate Ca^{2+} activity. GABA is synthesized and released by neuroblasts (Stewart et al., 2002; Nguyen et al., 2003; Bolteus and Bordey, 2004; De Marchis et al., 2004; Liu et al., 2005; Gascon et al., 2006) that may provide a tonic versus a phasic release of GABA (for review and discussion see Bordey, 2007). There are no known phasic or synaptic sources of GABA in the SVZ. It was suggested that ambient GABA levels may be in the μM range in the SVZ (Bolteus and Bordey, 2004; Bolteus et al., 2005). GABA levels are expected to fluctuate over time because neuroblasts migrate, thus changing the microenvironment of astrocyte-like cells. GABA$_A$ receptors in astrocyte-like cells have a reported EC_{50} for GABA of 15 μM and are thus expected to be tonically activated by low μM ambient GABA (Liu et al., 2005). Indeed, based on published data, GABA$_A$ receptors are tonically activated in 60% of the astrocyte-like cells (Liu et al., 2005). It was shown that bicuculline or picrotoxin applications induced a small shift in the current baseline that would correspond to a small depolarization of astrocyte-like cells.

Consistent with the predictions discussed above, we report that astrocyte-like cells of the SVZ display spontaneous Ca^{2+} transients, the activity of which is tonically regulated by ambient GABA acting on GABA$_A$ receptors. In particular, GABA$_A$ receptor inhibition revealed that tonic GABA$_A$ activation had two effects on SVZ astrocyte-like cells, dividing SVZ astrocytes into two functionally distinct populations. In one subpopulation of these cells, tonic GABA$_A$ receptor activation increased the frequency of Ca^{2+} transients while it decreased it in the other subpopulation. This latter GABA$_A$ action may result from a shunting effect of GABA$_A$ conductance in astrocyte-like cells. In future work, it will be important to understand how Ca^{2+} transients are generated in SVZ astrocytes.

In conclusion, tonic regulation of Ca^{2+} activity by ambient GABA could have major implications for the behavior of the Ca^{2+}-dependent release of diffusible molecules from astrocytes such as ATP (Striedinger et al., 2007). Considering that GABA$_A$ receptor activation has been shown to limit SVZ astrocyte proliferation (Liu et al., 2005), it remains to be determined whether GABA$_A$'s effect on proliferation involves L- and/or T-type VGCCs.

ACKNOWLEDGMENTS

This work was supported by grants from the National Institute of Health (NS048256 and DC007681, A.B.), Yale Brown-Coxe fellowship (J.-C.P.), and NRSA 1F31NS063758-01A1 (S.Z.Y.). We thank Tiffany Lin for assistance and discussion on the experiments and analysis. Thank you to M. Morgan Taylor for comments and editing.

SUPPLEMENTARY MATERIAL

The Supplementary Material for this article can be found online at http://www.frontiersin.org/cellularneuroscience/paper/10.3389/fncel.2010.00008/

REFERENCES

Barakat, L., and Bordey, A. (2002). GAT-1 and Reversible GABA Transport in Bergmann Glia in Slices. *J. Neurophysiol.* 88, 1407–1419.

Bekar, L. K., and Walz, W. (2002). Intracellular chloride modulates A-type potassium currents in astrocytes. *Glia* 39, 207–216.

Bellamy, T. C. (2006). Interactions between Purkinje neurones and Bergmann glia. *Cerebellum* 5, 116–126.

Bolteus, A. J., and Bordey, A. (2004). GABA Release and uptake regulate neuronal Precursor Migration in the Postnatal subventricular zone. *J. Neurosci.* 24, 7623–7631.

Bolteus, A. J., Garganta, C., and Bordey, A. (2005). Assays for measuring extracellular GABA levels and cell migration rate in acute slices. *Brain Res. Brain Res. Protoc.* 14, 126–134.

Bootman, M. D., Collins, T. J., Mackenzie, L., Roderick, H. L., Berridge, M. J., and Peppiatt, C. M. (2002). 2-aminoethoxydiphenyl borate (2-APB) is a reliable blocker of store-operated Ca2+ entry but an inconsistent inhibitor of InsP3-induced Ca2+ release. *FASEB J.* 16, 1145–1150.

Bordey, A. (2006). Adult neurogenesis: basic concepts of Signaling. *Cell Cycle* 5, 722–728.

Bordey, A. (2007). Enigmatic GABAergic networks in adult neurogenic zones. *Brain Res. Brain Res. Rev.* 53, 124–134.

Brenner, M., Kisseberth, W. C., Su, Y., Besnard, F., and Messing, A. (1994). GFAP promoter directs astrocyte-specific expression in transgenic mice. *J. Neurosci.* 14, 1030–1037.

Ciapa, B., Pesando, D., Wilding, M., and Whitaker, M. (1994). Cell-cycle calcium transients driven by cyclic changes in inositol trisphosphate levels. *Nature* 368, 875–878.

D'Andrea, P., Zacchetti, D., Meldolesi, J., and Grohovaz, F. (1993). Mechanism of [Ca2+]i oscillations in rat chromaffin cells. Complex Ca(2+)-dependent regulation of a ryanodine-insensitive oscillator. *J. Biol. Chem.* 268, 15213–15220.

De Marchis, S., Temoney, S., Erdelyi, F., Bovetti, S., Bovolin, P., Szabo, G., and Puche, A. C. (2004). GABAergic phenotypic differentiation of a subpopulation of subventricular derived migrating progenitors. *Eur. J. Neurosci.* 20, 1307–1317.

Doetsch, F., Petreanu, L., Caille, I., Garcia-Verdugo, J. M., and Alvarez-Buylla, A. (2002). EGF converts transit-amplifying neurogenic precursors in the adult brain into multipotent stem cells. *Neuron* 36, 1021–1034.

Fiacco, T. A., Agulhon, C., Taves, S. R., Petravicz, J., Casper, K. B., Dong, X., Chen, J., and McCarthy, K. D. (2007). Selective stimulation of astrocyte calcium in situ does not affect neuronal excitatory synaptic activity. *Neuron* 54, 611–626.

Gascon, E., Dayer, A. G., Sauvain, M. O., Potter, G., Jenny, B., De Roo, M., Zgraggen, E., Demaurex, N., Muller, D., and Kiss, J. Z. (2006). GABA regulates dendritic growth by stabilizing lamellipodia in newly generated interneurons of the olfactory bulb. *J. Neurosci.* 26, 12956–12966.

Lacinova, L. (2005). Voltage-dependent calcium channels. *Gen. Physiol. Biophys.* 24(Suppl. 1), 1–78.

Liu, X., Bolteus, A. J., Balkin, D. M., Henschel, O., and Bordey, A. (2006). GFAP-expressing cells in the postnatal subventricular zone display a unique glial phenotype intermediate between radial glia and astrocytes. *Glia* 54, 394–410.

Liu, X., Liao, D., and Ambudkar, I. S. (2001). Distinct mechanisms of [Ca2+]i oscillations in HSY and HSG cells: role of Ca2+ influx and internal Ca2+ store recycling. *J. Membr. Biol.* 181, 185–193.

Liu, X., Wang, Q., Haydar, T. F., and Bordey, A. (2005). Nonsynaptic GABA signaling in postnatal subventricular zone controls proliferation of GFAP-expressing progenitors. *Nat. Neurosci.* 8, 1179–1187.

Lledo, P. M., Alonso, M., and Grubb, M. S. (2006). Adult neurogenesis and functional plasticity in neuronal circuits. *Nat. Rev. Neurosci.* 7, 179–193.

Meier, S. D., Kafitz, K. W., and Rose, C. R. (2008). Developmental profile and mechanisms of GABA-induced calcium signaling in hippocampal astrocytes. *Glia* 56, 1127–1137.

Nguyen, L., Malgrange, B., Breuskin, I., Bettendorff, L., Moonen, G., Belachew, S., and Rigo, J. M. (2003). Autocrine/paracrine activation of the GABA(A) receptor inhibits the proliferation of neurogenic polysialylated neural cell adhesion molecule-positive (PSA-NCAM+) precursor cells from postnatal striatum. *J. Neurosci.* 23, 3278–3294.

Nielsen, J. V., Nielsen, F. H., Ismail, R., Noraberg, J., and Jensen, N. A. (2007). Hippocampus-like corticoneurogenesis induced by two isoforms of the BTB-zinc finger gene Zbtb20 in mice. *Development* 134, 1133–1140.

Nilius, B., Talavera, K., and Verkhratsky, A. (2006). T-type calcium channels: the never ending story. *Cell Calcium* 40, 81–88.

Noraberg, J., Jensen, C. V., Bonde, C., Montero, M., Nielsen, J. V., Jensen, N. A., and Zimmer, J. (2007). The developmental expression of fluorescent proteins in organotypic hippocampal slice cultures from transgenic mice and its use in the determination of excitotoxic neurodegeneration. *Altern. Lab. Anim.* 35, 61–70.

Owens, D. F., and Kriegstein, A. R. (2002). Is there more to GABA than synaptic inhibition? Nat. *Rev. Neurosci.* 3, 715–727.

Pathania, M., Yan, L. D., and Bordey, A. (2010). A symphony of signals conduct early and late stages of adult neurogenesis. Neuropharmacology.

Peppiatt, C. M., Collins, T. J., Mackenzie, L., Conway, S. J., Holmes, A. B., Bootman, M. D., Berridge, M. J., Seo, J. T., and Roderick, H. L. (2003). 2-Aminoethoxydiphenyl borate (2-APB) antagonises inositol 1, 4, 5-trisphosphate-induced calcium release, inhibits calcium pumps and has a use-dependent and slowly reversible action on store-operated calcium entry channels. *Cell Calcium* 34, 97–108.

Platel, J. C., Dave, K. A., and Bordey, A. (2008). Control of neuroblast production and migration by converging GABA and glutamate signals in the postnatal forebrain. *J. Physiol. (Lond.)* 586, 3739–3743.

Platel, J. C., Dupuis, A., Boisseau, S., Villaz, M., Albrieux, M., and Brocard, J. (2007). Synchrony of spontaneous calcium activity in mouse neocortex before synaptogenesis. *Eur. J. Neurosci.* 25, 920–928.

Platel, J. C., Gordon, V., Heintz, T., and Bordey, A. (2009). GFAP-GFP neural progenitors are antigenically homogeneous and anchored in their enclosed mosaic niche. *Glia* 57, 66–78.

Stewart, R. R., Hoge, G. J., Zigova, T., and Luskin, M. B. (2002). Neural progenitor cells of the neonatal rat anterior subventricular zone express functional GABA(A) receptors. *J. Neurobiol.* 50, 305–322.

Striedinger, K., Meda, P., and Scemes, E. (2007). Exocytosis of ATP from astrocyte progenitors modulates spontaneous Ca2+ oscillations and cell migration. *Glia* 55, 652–662.

Wang, D. D., Krueger, D. D., and Bordey, A. (2003a). Biophysical properties and ionic signature of neuronal progenitors of the postnatal subventricular zone in situ. *J. Neurophysiol.* 90, 2291–2302.

Wang, D. D., Krueger, D. D., and Bordey, A. (2003b). GABA depolarizes neuronal progenitors of the postnatal subventricular zone via GABA$_A$ receptor activation. *J. Physiol (Lond.)* 550, 785–800.

Zhao, C., Deng, W., and Gage, F. H. (2008). Mechanisms and functional implications of adult neurogenesis. *Cell* 132, 645–660.

Conflict of Interest Statement: The authors declare that the research was conducted in the absence of any commercial or financial relationships that could be construed as a potential conflict of interest.

Received: 02 February 2010; paper pending published: 03 March 2010; accepted: 10 March 2010; published online: 08 April 2010.

Citation: Young SZ, Platel J-C, Nielsen JV, Jensen NA and Bordey A (2010) GABA$_A$ increases calcium in subventricular zone astrocyte-like cells through L- and T-type voltage-gated calcium channels. Front. Cell. Neurosci. ***4****:8. doi: 10.3389/fncel.2010.00008*